JOURNAL OF MATERIALS SCIENCE **38** (2003) 1073–1079

Electric conductivity and oxygen permeability of modified cerium oxides

XIWANG QI, Y. S. LIN*
Department of Chemical Engineering, University of Cincinnati, Cincinnati, OH 45221-0171, USA
E-mail: jlin@alpha.che.uc.edu

C. T. HOLT, S. L. SWARTZ
NexTech Materials, Ltd., Worthington, OH 43085, USA

Electrical conductivities of samarium (Sm), terbium (Tb), praseodymium (Pr) and zirconium (Zr) doped ceria membranes were measured in $T = 600$–900°C and $pO_2 = 10^{-22}$–0.21 atm. Doping Sm and Pr in CeO_2 respectively enhances the ionic conductivity and electron-hole conductivity of ceria. Sm-Pr doped ceria exhibits both n-type (at lower pO_2) and p-type (at high pO_2) electronic and ionic conductivity in the temperature range studied. Adding Tb in the Sm doped ceria causes a reduction in ionic conductivity. Zr-Pr doped ceria is an n-type electronic conductor at low P_{O_2} and p-type electronic conductor at high pO_2. The ionic conductivity of Zr-Pr doped ceria is lower than Sm doped ceria but higher than pure ceria. Oxygen permeation flux through the Zr-Pr doped ceria membrane, dominated by the slow oxygen ionic conduction, is similar to the ytttria doped bismuth oxide membrane, and smaller, but close to that of perovskite-type lanthanum cobaltite membrane.

1. Introduction

Compared with other well known ionic conductors, such as fluorite structured zirconia [1, 2] and bismuth oxide [3, 4], ceria has perhaps the highest oxygen-ion mobility with a large solubility for acceptor doping [5, 6]. It has a variable-valent cation and an extensive range of nonstoichiometry. Pure CeO_2 shows n-type electronic conduction in a large range of the oxygen partial pressure (up to 1 atm) [6]. The oxygen ionic transference number is less than 0.2% in a large range of P_{O_2} (up to 1 atm) [6]. For example, at 600°C the oxygen ionic conductivity of pure CeO_2 is about 5×10^{-5} S/cm and the electronic conductivity is a few orders of magnitude larger than its ionic conductivity [7]. The electron-conduction in the pure ceria is associated with the electron-hoping between Ce^{4+} and Ce^{+3}. The ionic conduction in ceria is determined by the concentration of Ce^{+3} and the mobility of oxygen ions. Acceptor doping, with oxides such as Y_2O_3, increases the ionic conductivity of ceria at the expense of the electronic conductivity, resulting in predominant ionic conductivity at higher oxygen partial pressure [8].

Electronic conductivity in the ceria oxides is detrimental to their applications as solid oxide fuel cell electrolytes. For use as a membrane in air separation or membrane reactor systems, both high electronic (p-type) conductivity and high ionic (oxygen) conductivity are required. In present study, the effects of several dopants on the p-type electronic and oxygen ionic conductivity of ceria were investigated. The objective was to find a doped ceria material with high p-type electronic and high oxygen ionic conductivity in the P_{O_2} range of 10^{-6} to 0.21 atm. In this paper, we report on the preparation of ceria membranes doped with samarium (Sm), terbium (Tb), praseodymium (Pr) and zirconium (Zr). The electrical conductivity data were measured at various temperatures over a large range of oxygen partial pressures to examine how the dopant affects the electrical transport in ceria. Oxygen permeation through a representative membrane was measured to confirm the expected improvement in the oxygen permeability of the ceria membranes by the selected doping strategy.

2. Experimental

2.1. Membrane preparation

Hydrothermal synthesis was used to prepare the doped ceria ceramic powders. Hydrous oxide precursor gels were prepared by coprecipitation, and the gels were then reacted in an autoclave at temperatures of 200 to 250°C under autogenous pressure. Under these conditions, the hydrous oxide gels were converted into crystalline suspensions of nanoscale, crystalline solid-solution oxides. As-produced doped ceria powders had surface areas of ~150 m^2/gram. These powders were

*Author to whom all correspondence should be addressed.

then calcined at 800–900°C, to reduce surface area to the 20–30 m^2/gram range. The powders were formed into disks by isostatic pressing at 330 MPa and then sintered at 1300–1400°C for 2 hours to produce dense membranes.

2.2. Conductivity measurement

The four-point DC method was used in the measurement of the total conductivity of ceria under different temperatures and atmospheres. Ceria disks were machined into bars ($2.0 \times 6.0 \times 20$ mm) for this measurement. Four silver wires were connected to the ends of the sample bar by silver conductive paint. The sample was loaded into a quartz tube and heated by a tubular furnace, first to 900°C for 0.5 h. As a result, the silver paint formed continuous circular silver layers around the sample ends which act as electrodes. Then the furnace was cooled down to desired temperature for measurement. A stable direct electrical current was provided by PG201 Potentiostat (Radiometer A/S) to the sample bar through the two wires connected to the outer ends, and the voltage drop along the inner section of the bar was measured simultaneously through the two inner wires by B-845 Digital Multimeter (Protek).

During conductivity measurement, a continuous gas flow at a rate of 100 ml/min was introduced into the testing chamber. The oxygen partial pressure of the gas flow was adjusted by O_2/N_2 mixture in the range of 1×10^{-4}–1 atm and by CO/CO_2 mixture in the range below 1×10^{-10} atm. The oxygen content of the gas flow was measured by an oxygen analyzer (Series 6000, Illinois Instruments) with a resolution to 10^{-8} atm. In order to ensure steady state condition in the measurement, data were acquired at least 3 hrs or 30 min after gas concentration change or temperature change for O_2/N_2, and 5 hrs or 1 hr for CO/CO_2 atmosphere, respectively.

2.3. Oxygen permeation measurement

The oxygen permeation measurement system is shown in Fig. 1. The gas-tight ceria membranes with diameter of 25 mm were sealed by a ceramic sealant (50% strontium cerate, 40% Pyrex glass and 10% sodium aluminate) on the top of the inner dense alumina tube (2.54 cm in OD, from Coors Ceramics). This inner tube was inserted into a larger dense alumina tube (3.81 cm in OD, from Coors Ceramics). Air was introduced into the inner tube (served as upstream chamber) and helium was swept through the space between two alumina tubes (served as the downstream chamber).

In permeation experiment, the system was first heated to 950°C at which the membrane was sealed by the melted sealant. The nitrogen in the effluent of downstream was checked by a gas chromatograph (Perkin-Elmer) with a molecular sieve column (0.318 cm OD, 305 cm, 80/100 mesh, from Alltech) during the annealing step. After no nitrogen was detected in the helium flow, the system was cooled down at a rate of 5°C/min to 700°C to begin the oxygen permeation experiment. The oxygen concentration in the helium flow was measured by the same oxygen analyzer (series 6000, Illinois Instruments). The oxygen permeation fluxes through the membrane were calculated from the oxygen concentration and flow rate of the downstream effluent. In all cases, the gas flow rates passing through both chambers were kept at 50 ml/min. In this experiment, it took about 3 h to reach the steady-state oxygen permeation after air and helium were introduced into the permeation chambers and 1 h after any temperature changes.

3. Results and discussion

3.1. Membrane characteristics

The following ceria based ceramic membranes were prepared by the hydrothermal method: $Ce_{0.85}Sm_{0.15}O_{2-x}$ (CS), $Ce_{0.70}Pr_{0.30}O_{2-x}$ (CP), $Ce_{0.80}Sm_{0.10}Tb_{0.10}O_{2-x}$(CST), $Ce_{0.70}Sm_{0.10}Pr_{0.20}O_{2-x}$(CSP), $Ce_{0.60}Zr_{0.20}Pr_{0.20}O_{2-x}$(CZP). XRD analysis showed that all these samples had a fluorite FCC structure. Fig. 2 shows a TEM micrograph of the CS powder after calcination at 800–900°C followed by subsequent ball-milling to reduce agglomeration. As shown, the as synthesized ceria crystallites are in nanoscale, with a size in the range from 10–15 nm. All the sintered membranes had sintered densities exceeding 95% of the theoretical value. The membrane disks were gas-tight to helium as confirmed by gas permeation tests.

3.2. Electrical conductivity

The four-point DC method was used to measure the total conductivity, including both oxygen ionic and electronic conductivity. Nevertheless, the dependency of the total conductivity on the oxygen partial pressure

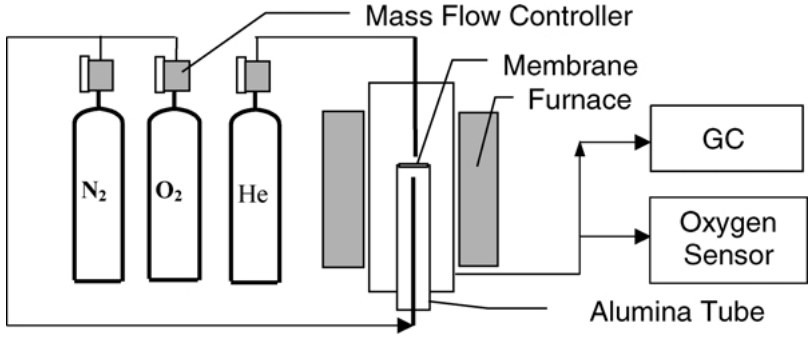

Figure 1 Schematic diagram of oxygen permeation measurement system.

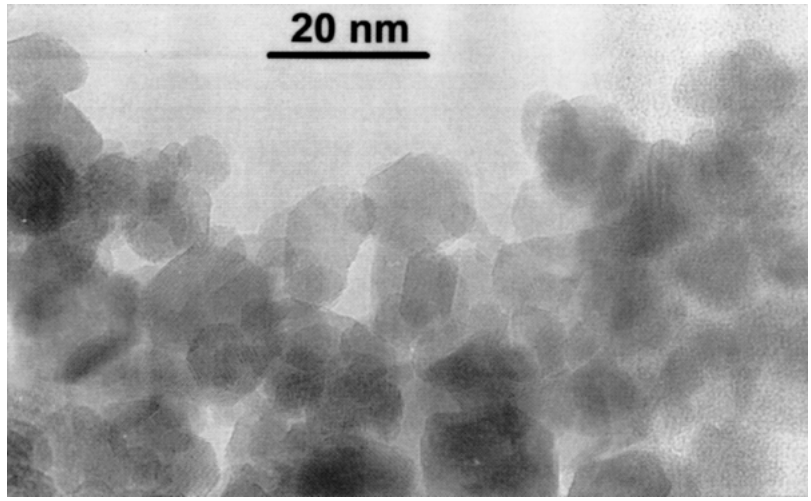

Figure 2 TEM micrograph of hydrothermally synthesized Sm doped ceria powder after calcinations at 800–900°C and ball-milling.

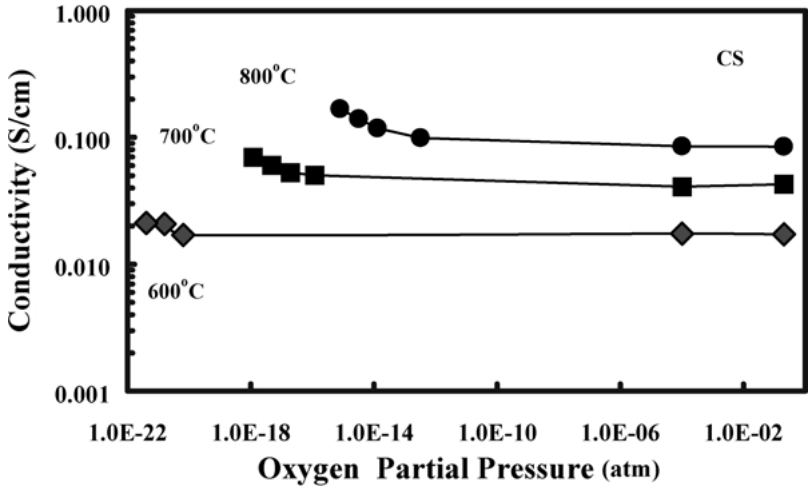

Figure 3 P_{O_2} dependence of total conductivity of $Ce_{0.85}Sm_{0.15}O_{2-x}$ (CS).

should give an indication of the dominant electrical transport mechanism. Fig. 3 shows the total conductivity of samarium (Sm) doped ceria, $Ce_{0.85}Sm_{0.15}O_{2-x}$ (CS), as a function of oxygen partial pressure at three different temperatures. In the higher oxygen partial pressure range, the conductivity is independent of pO_2, indicating a dominant oxygen ion conduction. The ionic conductivity at 800°C is about 0.1 S/cm, 2 to 3 times that of yttria stabilized zirconia (YSZ) membrane [8, 9]. At low pO_2 (below 10^{-12} atm), the electrical conductivity increases with decreasing pO_2, indicating the growing importance of the n-type electronic conduction in the low pO_2 range, especially at high temperature (800°C). The onset pO_2 for electronic conductivity shifts to higher pO_2 as the temperature is increased. The results show that Sm-doped ceria is an oxygen ionic conductor at high pO_2 and an n-type electronic conductor at low pO_2 in the temperature and P_{O_2} ranges studied.

Fig. 4 shows the electrical conductivity for praseodymium (Pr) doped ceria, $Ce_{0.70}Pr_{0.30}O_{2-x}$ (CP) in the conditions similar to those shown in Fig. 3. Different from the results given in Fig. 3, for CP an increase in electric conductivity with increasing pO_2 is noticeable in pO_2 from 10^{-21} to 10^{-3} atm, and this trend becomes more pronounced at pO_2 larger than 10^{-9} atm. These results indicate that the electronic-hole is the dominant conduction mechanism in CP over the entire range of conditions studied.

The present results show that doping Sm greatly enhances the ionic conductivity of ceria. For example, at 600°C the ionic conductivity of pure ceria is 5×10^{-5} S/cm whereas it is about 1.5×10^{-2} S/cm for the Sm-doped ceria, as shown in Fig. 3. Compared with pure ceria, the oxygen ionic, rather than electronic (n-type) conduction is dominant in the Sm-doped ceria at high pO_2 (10^{-10}–0.21 atm) because of the increase in the ionic conductivity. Doping with Sm does not appear to have an effect on the electronic conduction properties of ceria. In contrast, Pr doping in ceria significantly improves its electron-hole (p-type) conductivity. The Pr-doped ceria is essentially a p-type conductor in the entire P_{O_2} range studied. Doping with Pr may also increase the ionic conductivity of ceria but such effect is not clear from Fig. 4 because of the significantly enhanced electron-hole conduction.

Both Sm and Pr are within the lanthanide group with similar atomic structure. Sm has multiple oxidation states of +2 and +3, and Pr has primarily one oxidation

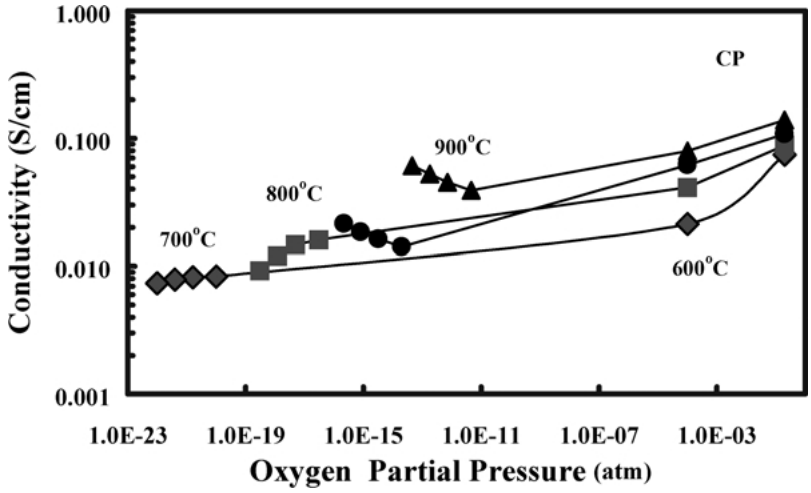

Figure 4 P_{O_2} dependence of total conductivity of $Ce_{0.70}Pr_{0.30}O_{2-x}$ (CP).

state of +3. For pure ceria the ionic conductivity is determined by the oxygen vacancy concentration, which is proportional to the concentration of Ce^{+3}. The presence of doped Sm at (+3), especially at lower oxidation state (+2), can increase drastically the oxygen vacancy concentration, raising the oxygen ionic conductivity as observed. Doping Pr with +3 oxidation state will increase the oxygen vacancy concentration, but to a much less extent as compared to Sm. It seems that the charge compensation for Pr doping is primarily electronic, making the Pr doped ceria a p-type electronic conductor.

Based on these results, binary Pr-Sm doping was applied in order to obtain a mixed oxygen ionic and p-type electronic conductor. Fig. 5 shows the conductivities of Pr-Sm doped ceria, $Ce_{0.7}Sm_{0.1}Pr_{0.2}O_{3-x}$ (CSP). Compared to the results shown in Figs 3 and 4, the electric conductivity curves of the Pr-Sm doped ceria sample seem to reassemble a combination of the conductivity curves for Sm doped ceria (Fig. 3) and Pr doped ceria (Fig. 4). For the CSP sample, the dominating conduction mechanism is electron conduction at low pO_2range and ionic conduction in the intermediate pO_2 range. The electronic-hole conduction in the CSP sample becomes important, but not as significant as the CP sample, at high pO_2 ($>10^{-4}$ atm).

Fig. 6 shows the electric conductivity data of the terbium and samarium doped ceria, $Ce_{0.80}Sm_{0.10}Tb_{0.10}O_{2-x}$(CST). The purpose of adding terbium was to improve the electronic (n-type) conductivity of Sm doped ceria to higher pO_2. However, compared with the results in Fig. 3, it is found that terbium modification actually lowered the conductivity of Sm-doped ceria by about 50 percent, both in the high and low oxygen partial pressure ranges, indicating that both oxygen ion and electronic conductivities were reduced. This suggests that the incorporation of Tb ions with higher valence (+3 and +4) reduces oxygen vacancy concentration and decreases the oxygen ion mobility within the lattice. It may also increase the difficulty of electronic charge transfer due to the high energy potential. Therefore, this modification did not achieve the desired results.

The electric conduction properties of $Ce_{0.6}Zr_{0.2}Pr_{0.2}O_{3-x}$ (CZP) are given in Fig. 7. The sample exhibits a dominant electronic (n-type) conduction at low pO_2 ($<10^{-12}$ atm) and electron-hole (p-type) conduction at high pO_2 ($>10^{-8}$ atm). Ionic conductivity of

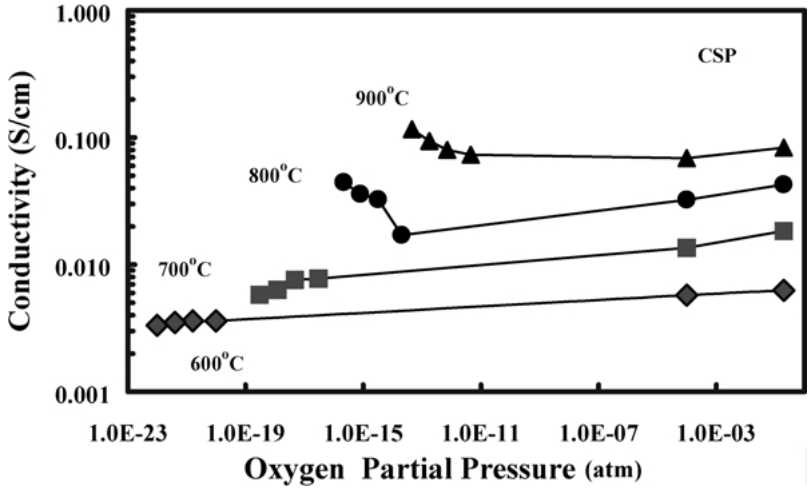

Figure 5 P_{O_2} dependence of total conductivity of $Ce_{0.70}Sm_{0.10}Pr_{0.20}O_{2-x}$ (CSP).

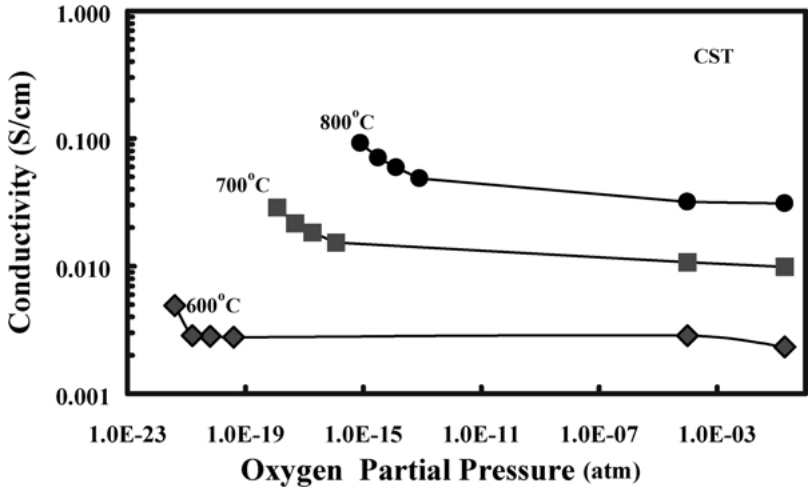

Figure 6 P_{O_2} dependence of total conductivity of $Ce_{0.80}Sm_{0.10}Tb_{0.10}O_{2-x}$ (CST).

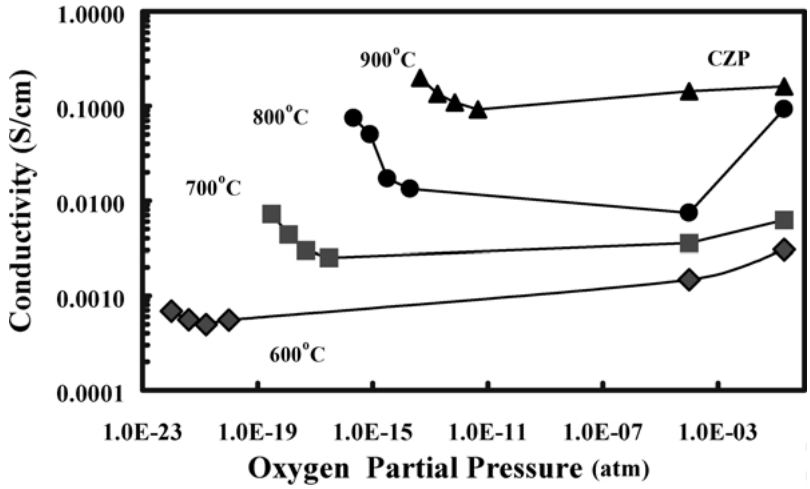

Figure 7 P_{O_2} dependence of total conductivity of $Ce_{0.60}Zr_{0.20}Pr_{0.20}O_{2-x}$ (CZP).

CZP could be much lower than that of Sm doped ceria, but would be higher than pure ceria. This is understandable as doping Zr, with an oxidation state of +4, would not increase the oxygen vacancy concentration of fluorite structured ceria. Compared with CSP sample, the CZP offers a higher n- and p- type electronic conductivity and much better mechanical strength.

3.3. Membranes and oxygen permeabilitiy

Materials to be used as the membrane for oxygen separation are preferred to have high ionic and electron-hole conductivities. CS and CTS exhibits appreciable electronic conductivity within the low oxygen partial pressure range. This makes them less attractive for use as the membrane material for oxygen separation application, where both faces of the membrane are exposed to oxidative atmospheres. Fig. 8 compares electric conductivity of three Pr doped cerium oxides: $Ce_{0.70}Pr_{0.30}O_{2-x}$ (CP), $Ce_{0.70}Sm_{0.10}Pr_{0.20}O_{2-x}$ (CSP), $Ce_{0.60}Zr_{0.20}Pr_{0.20}O_{2-x}$ (CZP) at 900°C. At high temperatures these three doped ceria oxides all exhibit both electron-hole conductivity (at high pO_2) and electron-conductivity (at low pO_2). The CZP membrane exhibited the highest electrical conductivity, and therefore it was expected that CZP would be a good membrane for oxygen separation at high temperatures.

The oxygen permeation rates through CZP membrane of 1 mm in thickness were then measured experimentally. The results are compared with that of a perovskite type membrane, $La_{0.8}Sr_{0.2}Co_{0.4}Fe_{0.6}O_3$ (LSCF), prepared by the spray-pyrolysis method [10], and fluorite structured membrane, $Bi_{1.5}Y_{0.5}O_3$ [11], both of 1.4 mm in thickness. Preparation of these membranes and their oxygen permeation measurements were also conducted in our laboratory. The comparison is given in Fig. 9.

As expected, the CZP membrane gives reasonable oxygen flux in the order of 1×10^{-8} mol/cm$^2 \cdot$ s. These flux data are 2 to 3 orders of magnitude larger than the zirconia based fluorite structured ceramic membranes [1], and are similar to bismuth oxide based ceramic membrane, as shown in the figure. The oxygen permeation flux of the CZP is comparable to the perovskite type LSCF ceramic membrane at the low temperature. CZP has a lower activation energy for oxygen permeation (46 kJ/mol) than the LSCF (132 kJ/mol). As a result, the oxygen permeation flux of CZP is lower than that of LSCF membrane at the higher temperatures, but close to that of yttrium

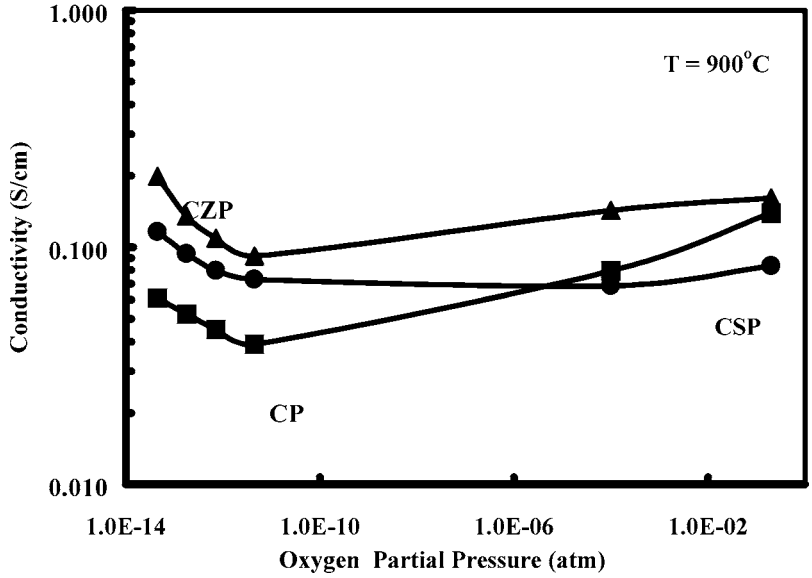

Figure 8 Comparison of electric conductivity of three Pr doped ceria samples.

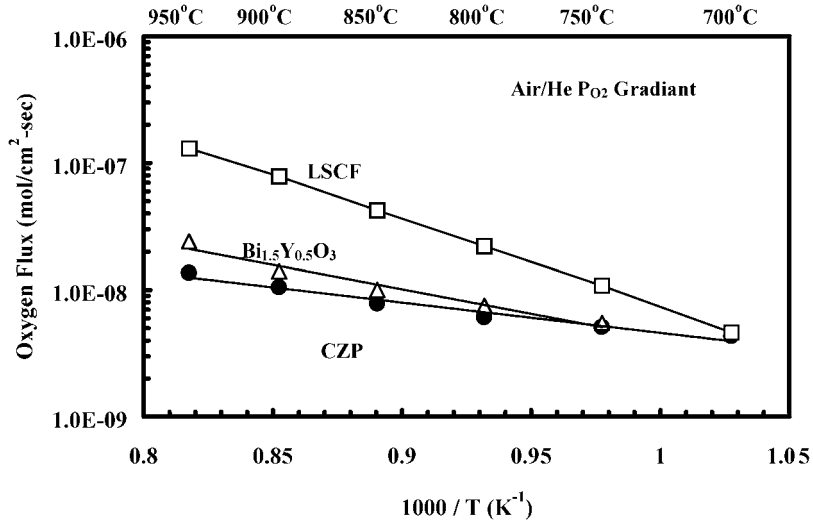

Figure 9 Comparison of oxygen permeation flux of CZP membrane (1 mm thick) with ($La_{0.}Sr_{0.2}Co_{0.4}Fe_{0.6}O_3$ (LSCF) and $Bi_{1.5}Y_{0.5}O_3$ (1.4 mm thick).

doped bismuth oxide membrane which has an intermediate activation energy of 70 kJ/mol for oxygen permeation.

It is known that the oxygen permeation flux is proportional to $[\sigma_e\sigma_i/(\sigma_e + \sigma_i)]$ [12]. LSCF and the bismuth oxide have an ionic transference number respectively close to 0 and 1. Therefore the oxygen permeation flux and associated activation energy for these two membranes are determined respectively by the oxygen ionic and electronic conduction. Arrhenius plots of the conductivity data for CZP given in Fig. 7 at different pO_2 yield an apparent activation energy for electric conduction in the range from 120–160 kJ/mol. This activation energy is much larger than the activation energy for oxygen permeation through CZP membrane (about 46 kJ/mol). It was reported that the activation energy for ionic conduction in the calcia doped ceria is in the range from 50–100 kJ/mol [6]. Thus, the activation energy for oxygen permeation through CZP is more close to that for ionic conduction in the ceria based membranes. The conductivity data given in Fig. 7 also show that the CZP is primarily an electronic conductor with ionic conductivity higher than pure ceria but still much lower than its own electronic conductivity. These indicate that the oxygen permeation through the CZP membrane is mainly controlled by the oxygen ionic conduction.

4. Conclusions

Compared to pure ceria, Sm-doped ceria remains as an n-type electronic conductor at low pO_2. However, doping Sm increases ionic conductivity, making Sm-doped ceria an ionic conductor at high pO_2 ($>10^{-10}$ atm). Doping of ceria with Pr increases the electron-hole conductivity. Adding Tb in the Sm doped ceria lowers its ionic conductivity but the Tb and Sm doped ceria remains as an n-type electronic conductor at low pO_2. The electric conduction properties of Sm-Pr co-doped ceria resembles a combination of Sm-doped ceria and Pr-doped ceria.

Zr-Pr doped ceria (CZP) shows appreciable n-type (at low pO_2) and p-type electronic (at high pO_2)

conduction. The CZP membrane exhibits a reasonable oxygen flux, comparable to the perovskite type membrane at lower temperature (700°C) and yttria doped bismuth oxide membranes in the entire temperature range studied (700–950°C). The activation energy data suggests that the oxygen permeation in CZP membrane is limited by the oxygen ionic conduction.

References

1. J.-H. PARK and R. B. BLUMENTHAL, *J. Electrochemi. Society* **136** (1989) 2869.
2. J. KIM and Y. S. LIN, *J. Membrane Science* **139** (1998) 75.
3. J. R. JURADO, C. MOURE, P. DURAN and N. VALVERDE, *Solid State Ionics* **28–30** (1988) 518.
4. H. J. M. BOUWMEESTER, H. KRUIDHOF, A. J. BURGGRAAF and P. J. GELLINGS, *ibid.* **53–56** (1992) 460.
5. M. PAN, G. Y. MENG, H. W. XIN, C. S. CHEN, D. K. PENG and Y. S. LIN, *Thin Solid Films* **324** (1998) 89.
6. M. MOGENSEN, N. M. SAMMES and G. A. TOMPSETT, *Solid State Ionics* **129** (2000) 63.
7. W. HUANG, P. SHUK and M. GREENBLATT, *ibid.* **100** (1997) 23.
8. H. L. TULLER, *ibid.* **52** (1992) 135.
9. J. KIM and Y. S. LIN, *J. Amer. Ceram. Soc.* **82** (1999) 2641.
10. X. QI, Y. S. LIN and S. L SWARTZ, *Ind. Eng. Chem. Res.* **39** (2000) 646.
11. Y. ZENG and Y. S. LIN, *J. Catalysis* **193** (2000) 58.
12. Y. S. LIN, W. WANG and J. HAN, *AIChE J.* **40** (1994) 786.

Received 11 April 2001
and accepted 17 October 2002